Acta Astronautica 188 (2021) 362–366

Contents lists available at ScienceDirect

Acta Astronautica

journal homepage: www.elsevier.com/locate/actaastro

Improvement of the electron beam (e-beam) lunar dust mitigation technology with varying the beam incident angle

B. Farr [a,b], X. Wang [a,b,*], J. Goree [c], I. Hahn [d], U. Israelsson [d], M. Horányi [a,b]

[a] Laboratory for Atmospheric and Space Physics, University of Colorado, Boulder, CO, 80303, USA
[b] NASA/SSERVI's Institute for Modeling Plasma, Atmospheres and Cosmic Dust, Boulder, CO, 80303, USA
[c] Department of Physics and Astronomy, University of Iowa, Iowa City, IA, 52242, USA
[d] Jet Propulsion Laboratory, California Institute of Technology, Pasadena, CA, 91109, USA

A B S T R A C T

Dust hazards are considered to be one of the technical challenges for future lunar exploration. In our past work a new dust mitigation technology was introduced utilizing an electron beam to remove dust particles from various surfaces. This technology was developed based on a patched charge model, which shows that the emission and re-absorption of electron beam induced secondary electrons inside microcavities between dust particles can lead to sufficiently large charges on the dust particles, causing their release from the surface due to strong repulsive forces. In this paper an improvement in the effectiveness of this technology is demonstrated with varying the beam incident angle on dust-covered sample surfaces by rotating the samples relative to the beam. Due to random arrangements of the microcavities, more of them will be exposed to the beam with various incident angles, thereby causing more dust release from the surface. The cleaning performance is tested against three samples: glass, spacesuit, and a photovoltaic (PV) panel. Lunar simulant (<25 μm in diameter) is deposited onto the sample surfaces such that the initial cleanliness of the samples is 0 % (full dust coverage) and 40 %. Varying the beam incident angle shows an overall surface cleanliness increase of 10–20 % in addition to the cleanliness achieved with a fixed beam angle. The ultimate cleanliness reaches 83–92 % for the glass and spacesuit samples. The PV panel coated with MgF_2 is shown to be more adhesive to the dust with the maximum cleanliness of 50–63 %.

1. Introduction

Lunar dust has been recognized as an issue for human exploration since the Apollo era. The dust can be stirred up due to robotic and/or human activities or released by natural processes such as micrometeoroid impacts and electrostatic lofting. As learned from the Apollo missions, lunar dust can readily stick to all surfaces, causing damages to spacesuits [1], degradation of thermal radiators and optical components [2–6], and failures of mechanisms [7]. In addition, lunar dust in human living quarters could lead to health risks when inhaled by astronauts [8,9]. Dust mitigation is needed to ensure the success of future human and robotic exploration, especially the long-term presence on the lunar surface. Different types of lunar dust mitigation technologies have been developed over the past decades [10]. These technologies include fluidal (e.g., liquid jet, foams or compressed gases) [11–13], mechanical (e.g., brushing or vibrating) [4,5], electrodynamic (e.g., the Electrodynamic Dust Shield and a photovoltaic dust removal electrode) [14–22] and passive (e.g., surface modification for reduced adhesion) [5,23–25] methods. These methods have both advantages and disadvantages, and their selection depends on the dust characteristics, surface properties, and application scenarios.

Recently, a new technology utilizing an electron beam (e-beam) to remove dust particles from various surfaces has been developed [26]. This e-beam technology aims to clean fine lunar dust (smaller than a few tens of microns in diameter), which has been discovered from the returned Apollo samples [27,28]. Finer dust particles are expected to be "stickier" due to their stronger adhesive and electrostatic forces, causing their mitigation to be more challenging. Therefore, finer lunar dust is expected to pose a higher risk to human and robotic exploration. Our e-beam technology was demonstrated using lunar simulant <25 μm in diameter. Optimal beam parameters have been found to be ~230 eV beam energy and >1.5 $\mu A/cm^2$ current density. Both spacesuit and glass sample surfaces with 40 % initial cleanliness (i.e., 60 % dust coverage) were shown to achieve 75–85 % cleanliness on a beam exposure timescale of ~100 s [26].

Earlier work has shown that introducing an electron beam to a dust-covered surface can cause dust particles to be charged and released from the surface due to electrostatic forces [29–31]. However, explaining this dust release mechanism was not possible using previous charging theories [29,30,32,33]. A recently developed patched charge model has provided a new insight into the fundamentals of the dust charging and release process [34]. The model suggests that microcavities are formed

* Corresponding author. Laboratory for Atmospheric and Space Physics, University of Colorado, Boulder, CO, 80303, USA.
E-mail address: xu.wang@colorado.edu (X. Wang).

https://doi.org/10.1016/j.actaastro.2021.07.040
Received 9 April 2021; Received in revised form 11 July 2021; Accepted 27 July 2021
Available online 31 July 2021

between dust particles, and the emission and re-absorption of secondary electrons generated by energetic electron impacts inside the microcavities can result in a buildup of large negative charges on the surrounding dust particles due to an intense electric field created across a small cavity. Subsequent strong electric repulsive forces between these negatively charged particles lead to their release from the surface. This model is supported by several follow-up experiments [e.g., 34–39]. Based on this patched charge model, the e-beam dust mitigation technology was developed and used in a well-controlled manner [26].

In this work, we demonstrate an improvement in the effectiveness of the e-beam technology of Ref. [26]. In the physical description of the patched charge model, microcavities are expected to be randomly arranged between dust particles such that their openings are oriented in different directions (Fig. 1). Only electron beams with particular incident angles can reach into the corresponding microcavities, as illustrated in Fig. 1 with green, blue and red beam lines. Thus, we hypothesize that varying the electron beam incident angle relative to a dust-covered surface will expose more microcavities to the beam, thereby causing more dust particles to be sufficiently charged by beam-induced secondary electrons and released from the surface [34].

This hypothesis was tested and confirmed in our experimental demonstration in which the beam incident angle was varied by rotating the sample surfaces relative to the beam. The following sections show the experimental method and results on the improvements of the cleaning effectiveness in addition to the samples being cleaned at a fixed beam incident angle [26].

2. Experimental setup and method

The experiment was carried out in a 50 cm diameter and 28 cm tall vacuum chamber (Fig. 2). JSC-1 lunar simulant (ρ ~2.9 × 10^3 kg/m^3, <25 μm in diameter) was uniformly deposited on a test sample (2.5 cm × 5 cm) attached on a substrate at the end of a shaft. The deposition procedure is described in detail in our prior work [26]. The sample surface was exposed to an electron beam emitted from a negatively biased hot filament mounted on the top of the chamber. The beam at the source was ~5 cm diameter and ~20 cm above the sample surface, creating an approximately uniform beam spot on the sample surface. The substrate shaft was connected to a motor that continuously rotates the sample at a slow rate of 6 rpm such that the electron beam is incident

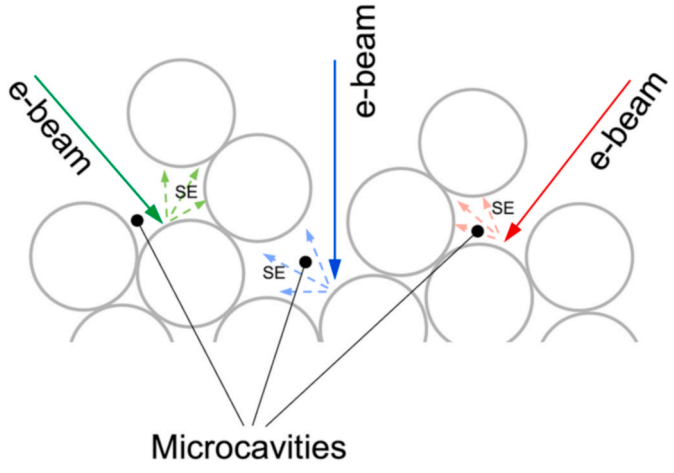

Fig. 1. Schematic of microcavity configurations as an example. Each microcavity can only allow an electron beam (green, blue or red) with a particular angle to enter, generating secondary electrons (SE) inside the microcavity. The SEs deposit and accumulate large negative charges on the surfaces of the surrounding dust particles of each microcavity, causing them to repel each other and be released from the surface [34]. Varying the beam angle allows more microcavities to be exposed to the beam and subsequently causes more dust to come off the surface.

on the sample surface at angles between 0° and 180°. As shown in Fig. 2a, the electron beam source was modified from our prior configuration [26] by installing a grounded grid a few millimeters below the filament to create an electric field to accelerate emitted electrons from the filament. This electric field eliminates the space charge effect near the filament, creating high beam currents without the need of a plasma, which was generated with argon gas at a neutral pressure of ~0.2 mTorr in our prior work [26]. The beam energy and current density at the sample surface were 230 eV and 1.5 μA/cm^2, respectively, which are the optimized parameters for an effective cleaning process [26]. A regular-speed video camera was used to record the initial surface cleanliness and its changes throughout the cleaning process.

As described in our prior work [26], the surface cleanliness defines the dust coverage of the test sample surface (the lower the cleanliness the higher the dust coverage). In our experiments, the surface cleanliness C is conveniently defined as [26].

$$C = (L_s - L_d)/(L_c - L_d) \quad (1)$$

where L_s is the average pixel brightness of the sample surface at a certain point during the cleaning process, L_c is the average pixel brightness of the clean surface (no dust), and L_d is the average pixel brightness of the surface fully covered by dust. All images were taken through the same vacuum chamber glass window with same lighting conditions to ensure the imaging consistency throughout the cleaning process.

The effect of varying the beam incident angle on dust removal was tested to verify the hypothesis described in Section 1. As in our prior work [26], a dust-covered sample surface was initially positioned at 45° to the electron beam and underwent the dust removal process until the process stopped. The sample was then rotated ~10°. Dust release was revived and then died down as shown from motions of dust jumping off the surface recorded using a high-speed video camera at 2000 fps. This process was repeated with the sample rotated to different angles, showing that variations of the beam incident angle cause more dust to come off the surface. This observation shows agreement with our hypothesis.

As a control, we also tested rotation for all sample surfaces, including the ones with full dust coverage (i.e., 0 % cleanliness), without turning on the electron beam. We found no noticeable dust falling off the surface due to gravity and rotation-caused vibration.

Anticipating the practical application of our technology, we note that rotation was used to vary the relative angle between the sample surface and the electron beam due to its relatively easy implementation for lab testing. For lunar applications, instead of rotation, a set of electron beam sources can be arranged at different angles, or a movable or portable beam source can be pointed at various angles relative to a surface area being cleaned to maximize the cleaning performance.

A full cleaning process was performed in two steps. First the sample surface was held stationary at 45° relative to the electron beam until the cleaning process stopped, then the rotation started and continued until the maximum cleanliness was reached. Additional cleanliness improvements were observed by comparing the results between the first and second steps. Periodically during rotation, the sample surface was stopped at 45° to take images for consistent data analysis.

Three sample materials were tested, including glass, spacesuit, and a photovoltaic (PV) panel. The spacesuit material was Apollo-era fabric, obtained in 2005 from Johnson Space Center. The glass and spacesuit materials were used in our prior work with a fixed sample position at 45° relative to the electron beam. The PV panel is a new sample tested in this experiment. The PV panel surface is coated with a layer of MgF_2, which is an anti-reflective material. Each of the sample surfaces was tested with two different initial cleanliness levels: 0 % (full dust coverage) and 40 %. As described in Ref. [26], the cleanliness level also correlates to the thickness of the dust layer as dust likely clumps together and accumulates multiple layers during its deposition. The lower surface cleanliness corresponds to a thicker layer of dust and vice versa. It was shown that

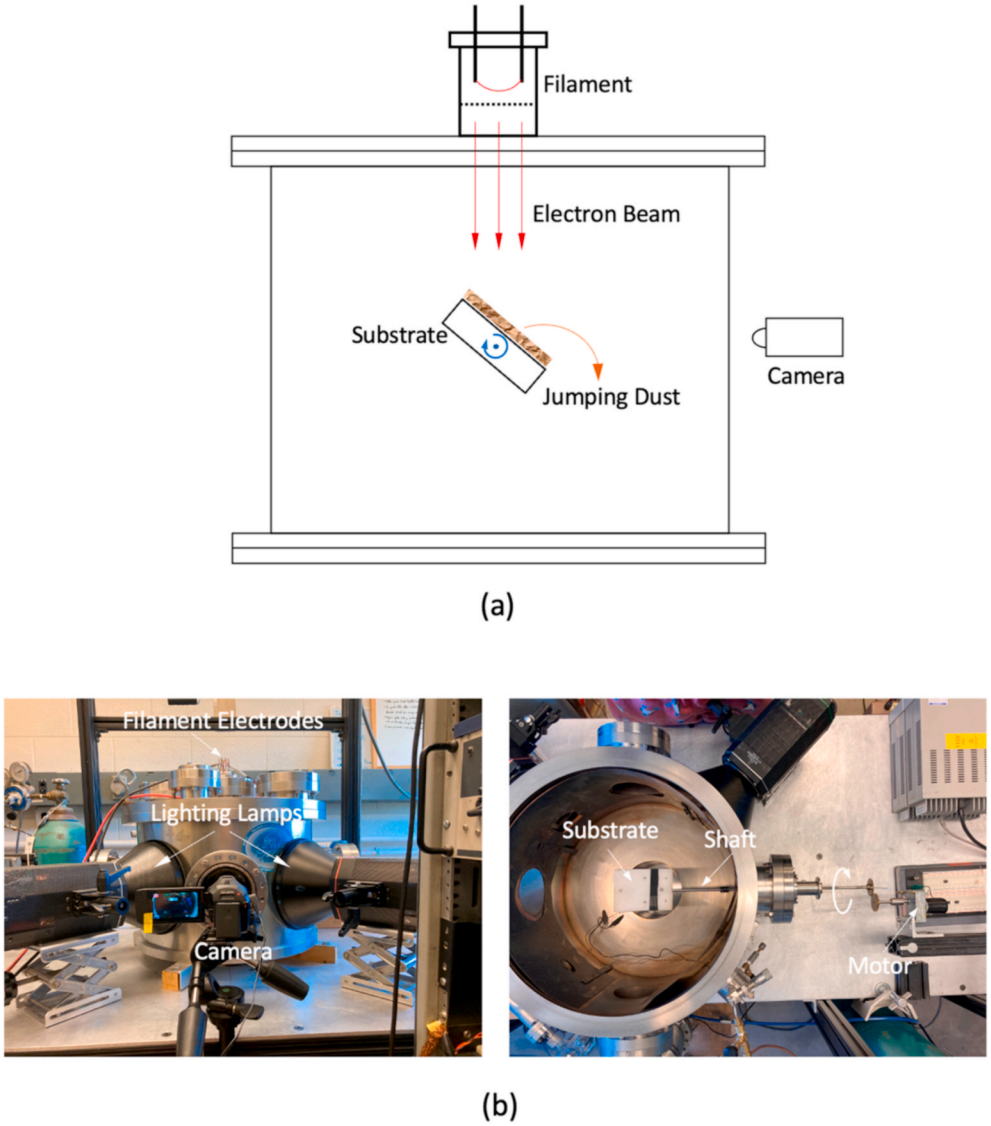

Fig. 2. a) Schematic of the experimental setup. An electron beam is generated using a negatively biased hot filament on the top of the chamber. A grounded grid is installed a few millimeters below the filament to create an electric field to accelerate the emitted electrons. For all the tests, the electron beam energy and current density are 230 eV and 1.5 μA/cm^2, respectively. Samples are attached to a substrate and deposited with lunar simulant (JSC-1, <25 μm in diameter). The substrate is attached to a shaft that is rotated at a rate of 6 rpm (blue circular arrow) by a motor. A video camera is used to record cleanliness changes of the sample surface over the course of the cleaning process; and b) Photographs of the experimental chamber setup. (For interpretation of the references to colour in this figure legend, the reader is referred to the Web version of this article.)

the dust layer thickness is expected to affect cleaning results [26]. Each of the tests included 3–4 trials, and their averaged results are shown in Figs. 3–5 with the standard deviations as error bars.

3. Results and discussion

Figs. 3–5 show the cleanliness as a function of time as both cleaning steps were completed for three samples. The sample surfaces were tested with two initial cleanliness levels of 0 % and 40 %, which also correspond to thick and thin dust layers, respectively.

In Fig. 3a, a glass sample fully covered by dust (i.e., 0 % cleanliness) is shown to reach ~65 % cleanliness while the sample was held stationary, and the subsequent rotation of the sample increased the cleanliness to ~85 %, showing a ~20 % improvement. The glass sample starting with 40 % cleanliness reached as high as ~88 % cleanliness while the sample was held stationary, and the subsequent rotation only yielded an additional 4 % to give an overall cleanliness of ~92 %. The size distribution of remaining dust particles after the full cleaning process was analyzed by placing the glass sample under a microscope. Fig. 3b shows that the remaining dust particles are mostly smaller ones with sizes <10 μm. Their cumulative cross-section covered ~9 % of the total analyzed area, meaning that the surface cleanliness is ~91 %, in agreement with the brightness analysis results.

Fig. 4 shows that the cleanliness of a spacesuit sample starting with 0 % and 40 % reached ~53 % and ~67 %, respectively, after cleaning with the sample being held stationary. Rotating the sample increased the cleanliness to ~83 % in both cases, resulting in 16–30 % improvements.

The significant improvements by rotation, for the spacesuit surface, may be related to its rough surface morphology. The woven fabric has small pocket-like features. On the one hand, these features can trap dust particles. On the other hand, microcavities can be formed between the dust particles and pockets, allowing more dust being sufficiently charged and released when the beam is directed at various angles to reach into these cavities.

Fig. 5 shows that a PV panel with full dust coverage (i.e., 0 % cleanliness) reached ~40 % cleanliness after exposure to the electron beam, and rotating the sample increased the overall cleanliness to ~50 %, showing a ~10 % improvement. The sample with 40 % cleanliness achieved ~63 % cleanliness after beam exposure, rotating the sample yielded little to no additional cleaning. The PV panel was found to be more difficult to be cleaned than the glass and spacesuit samples, indicating that its outmost layer of MgF_2 is more adhesive to dust. The underlying reason for this difference is uncertain.

Our results show that, for most cases, rotating the samples relative to the electron beam can result in removal of more dust to increase the surface cleanliness by 10–20 % on average in addition to the cleanliness

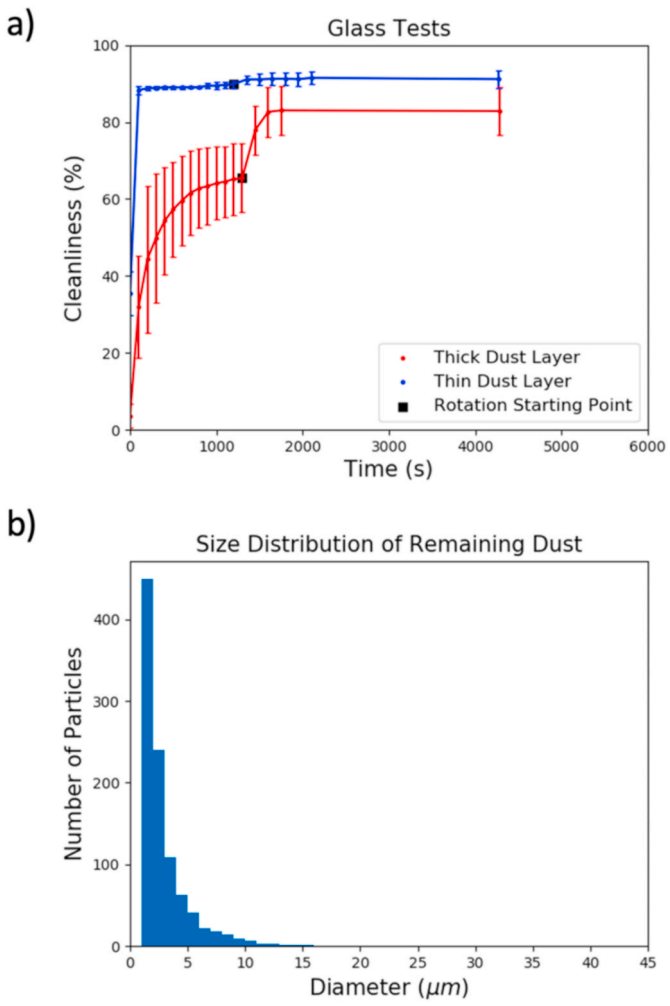

Fig. 3. a) The cleanliness as a function of time for a glass sample with 0 % (full dust coverage) and 40 % initial cleanliness, corresponding to thick and thin initial dust layers, respectively. The cleaning process started with the sample held stationary 45° relative to the electron beam followed by rotation as indicated by black squares. b) Size distribution of remaining dust particles after the full cleaning process. It shows that the remaining dust particles were the finer ones <10 μm, and the larger ones between 10 and 25 μm were mostly removed.

reached with the samples being held stationary. This effect was mostly noticeable during the spacesuit tests. Both the stationary and rotating cleaning processes achieved their maximum cleanliness levels on the timescale of a few minutes or less. Additionally, the thickness of initial dust layers showed an effect on the cleaning performance, which is more pronounced for the samples held at a fixed angle to the beam. Similar to the results shown in Ref. [26], thicker layers were found to result in the lower final cleanliness, possibly due to their higher dust compactness as a result of gravity and the subsequently decreased microcavity charging efficiency. It was shown in this work that varying the beam incident angle reduces the effect of the initial dust layer thickness on the overall cleaning performance.

4. Conclusion

An improvement of the e-beam dust removal technology [26] was demonstrated by varying the beam incident angle on sample surfaces by rotating the samples relative to the beam. The idea was based on the patched charge model [34]. Microcavities are expected to be randomly organized between dust particles, and variations of the beam incident angle will allow more microcavities to be exposed to the beam, thereby

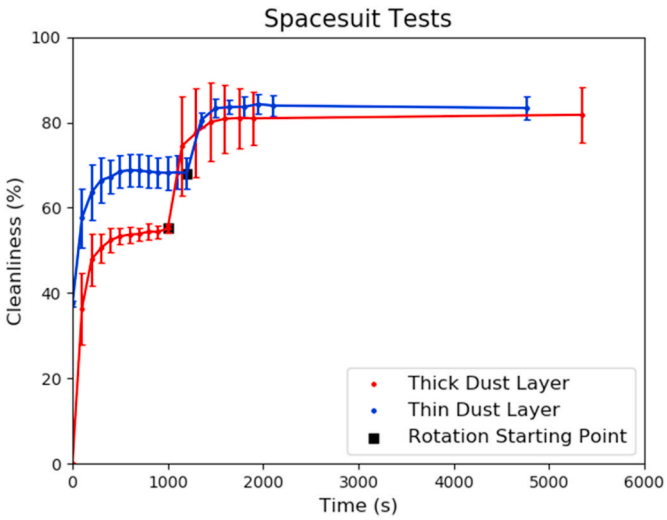

Fig. 4. The cleanliness as a function of time for a spacesuit sample. The initial surface cleanliness levels and corresponding thicknesses of the dust layers, as well as the cleaning procedure were the same as described in Fig. 3.

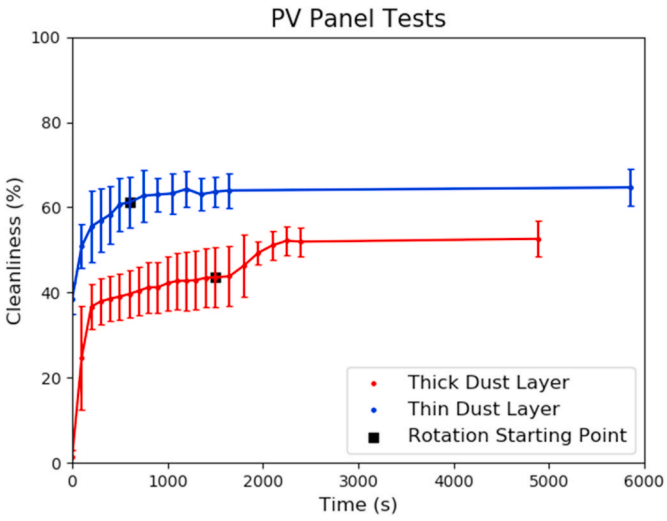

Fig. 5. The cleanliness as a function of time for a PV panel sample. The initial surface cleanliness levels and corresponding thicknesses of the dust layers, as well as the cleaning procedure were the same as described in Fig. 3.

causing more dust particles to be sufficiently charged by beam-induced secondary electrons and subsequently released from the surface due to strong repulsive forces. It was recorded that additional dust came off the surface as the beam incident angle was changed.

The cleaning performance was tested against three samples: glass, spacesuit and a PV panel. Lunar simulant <25 μm in diameter was deposited on the surfaces of the samples with initial cleanliness levels of 0 % (full dust coverage) and 40 %, which also correspond to thick and thin dust layers. The cleaning began with the sample surfaces held stationary at 45° relative to the beam, followed by rotation to vary the beam incident angle. It was shown that for most cases varying the beam incident angle increased the final cleanliness by 10–20 % on average after the samples were cleaned at a fixed beam angle. This effect was most significant for the spacesuit surface. It was shown that thicker dust layers reached a lower final cleanliness than thinner layers, as also demonstrated in our prior work [26], but their differences were reduced after cleaning with varying the beam incident angle. The overall maximum cleanliness reached 83–92 % for the glass and spacesuit samples. The PV panel coated with MgF_2 was demonstrated to be more

adhesive to the dust with the maximum cleanliness of 50–63 %.

For lunar applications, one can either configure multiple e-beam sources with different beam angles or have a movable or portable beam source to point at various angles to maximize the dust cleaning effectiveness. Such configurations will be tested in future experiments. Additionally, future work will include the testing of a variety of samples, including Kapton, Indium-tin-oxide (ITO), camera lenses and metals to examine the versatility of this technology.

Declaration of competing interest

The authors declare that they have no known competing financial interests or personal relationships that could have appeared to influence the work reported in this paper.

Acknowledgements

The authors thank Joel Schwartz for providing the sample PV panel used in the test. This work was supported by NASA/BPS and the Game Changing Development Dust Mitigation project through a contract with the Jet Propulsion Laboratory, California Institute of Technology, and by the NASA/SSERVI's Institute for Modeling Plasma, Atmospheres and Cosmic Dust (IMPACT).

References

[1] R. Goodwin, Apogee Books, Apollo 17: The NASA Mission Reports 1 (2002). ON, Canada, 2002.
[2] T.W. Murphy, E.G. Adelberger, J.B.R. Battat, C.D. Hoyle, R.J. McMillan, E. L. Michelsen, R.L. Samad, C.W. Stubbs, H.E. Swanson, Long-term degradation of optical devices on the Moon, Icarus 208 (2010) 31–35.
[3] T.W. Murphy, R.J. McMillan, N.H. Johnson, S.D. Goodrow, Lunar eclipse observations reveal anomalous thermal performance of Apollo reflectors, Icarus 231 (2014) 183–192.
[4] J.R. Gaier, K. Journey, S. Christopher, S. Davis, Evaluation of Brushing as a Lunar Dust Mitigation Strategy for Thermal Control Surfaces, 2011, p. 2011. NASA/TM-2011-217231/AIAA-2011-5182.
[5] J.R. Gaier, D.L. Waters, R.M. Misconin, B.A. Banks, M. Crowder, Evaluation of Surface Modification as a Lunar Dust Mitigation Strategy for Thermal Control Surfaces, 2011, p. 2011. NASA/TM-2011-217230/AIAA-2011-5183.
[6] C.M. Katzan, D.J. Brinker, R. Kress, The Effects of Lunar Dust Accumulation on the Performance of Photovoltaic Arrays, Space Photovoltaic Research and Technology Conference, NASA Lewis Research Center, Cleveland, Ohio, 1991, 1991.
[7] J.R. Gaier, The Effects of Lunar Dust on EVA Systems during the Apollo Missions, 2005, p. 2005. NASA/TM-2005-213610.
[8] D.G. Schrunk, B.L. Sharpe, B.L. Cooper, M. Thangavelu, The Moon: Resources, Future Development and Colonization, Praxis Publishing Ltd., Chichester, 1999, 1999.
[9] J.T. James, N. Khan-Mayberry, Risk of Adverse Health Effects from Lunar Dust Exposure, the Human Research Program Evidence Book, 2009, p. 2009. NASA-SP-2009-3045.
[10] N. Afshar-Mohajer, C.-Y. Wu, J.S. Curtis, J.R. Gaier, Review of dust transport and mitigation technologies in lunar and Martian atmospheres, Adv. Space Res. 56 (2015) 1222–1241.
[11] F. Tatom, V. Srepel, R. Johnson, N. Contaxes, J. Adams, H. Seaman, B. Cline, Lunar Dust Degradation Effects and Removal/prevention Concepts, 1967, p. 1967. NASA Technical Report No. TR-792-7-207A, 3-1.
[12] R.V. Peterson, C.W. Bowers, Contamination removal by CO2 jet spray, in: Proc. Optical System Contamination: Effects, Measurement, Control II, International Society for Optics and Photonics, 1990, pp. 72–85.
[13] K. Wood, Design of Equipment for Lunar Dust Removal, 1991, p. 1991. NASA-CR-190014.
[14] R. Sims, A. Biris, J. Wilson, C. Yurteri, M. Mazumder, C. Calle, C. Buhler, Development of a transparent self-cleaning dust shield for solar panels, Proc. ESA – IEEE Joint Meet, Electrostat (2003) 814–821.
[15] C. Calle, M. Mazumder, C. Immer, C. Buhler, J. Clements, P. Lundeen, A. Chen, J. G. Mantovani, Electrodynamic Dust Shield for Surface Exploration Activities on the Moon and Mars, 2006, p. 2006. IAC-06-A5.2.07.
[16] C. Calle, C. Buhler, J. McFall, S. Snyder, Particle removal by electrostatic and dielectrophoretic forces for dust control during lunar exploration missions, J. Electrost. 67 (2009) 89–92.
[17] C. Calle, C. Buhler, M. Johansen, M. Hogue, S. Snyder, Active dust control and mitigation technology for lunar and Martian exploration, Acta Astronaut. 69 (2011) 1082–1088.
[18] K.K. Manyapu, P.D. Leon, L. Peltz, J.R. Gaier, D. Waters, Proof of concept demonstration of novel technologies for lunar spacesuit dust mitigation, Acta Astronaut. 137 (2017) 472–481.
[19] H. Kawamoto, S. Hashime, Practical performance of an electrostatic cleaning system for removal of lunar dust from optical elements utilizing electrostatic traveling wave, J. Electrost. 94 (2018) 38–43.
[20] J. Jiang, Y. Lu, X. Yan, L. Wang, An optimization dust-removing electrode design method aiming at improving dust mitigation efficiency in lunar exploration, Acta Astronaut. 166 (2020) 59–68.
[21] J. Jiang, Y. Lu, H. Zhao, L. Wang, Experiments on dust removal performance of a novel PLZT driven lunar dust mitigation technique, Acta Astronaut. 165 (2019) 17–24.
[22] Y. Lu, J. Jiang, X. Yan, L. Wang, A new photovoltaic lunar dust removal technique based on the coplanar bipolar electrodes,, Smart Mater. Struct. 28 (2019), 085010.
[23] A. Dove, G. Devaud, X. Wang, M. Crowder, A. Lawitzke, C. Haley, Mitigation of lunar dust adhesion by surface modification, Planet. Space Sci. 59 (2011) 1784–1790.
[24] J.R. Gaier, Interpretation of the Apollo 14 thermal degradation sample experiment, Icarus 221 (2012) 167–173.
[25] J.R. Gaier, P. Berkebile, Implication of adhesion studies for dust mitigation on thermal control surfaces, in: AIAA Aerospace Sciences Meeting, 2012, p. 2012. AIAA-2012-0875.
[26] B. Farr, X. Wang, J. Goree, I. Hahn, U. Israelsson, M. Horányi, Dust mitigation technology for lunar exploration utilizing an electron beam, Acta Astronaut. 177 (2020) 405–409.
[27] J.C. Graf, Lunar soils grain size catalog, NASA Ref. Publ. 1265 (1993).
[28] J. Park, Y. Liu, K.D. Kihm, L.A. Taylor, Characterization of lunar dust for toxicological studies I: particle size distribution, J. Aero. Eng. 21 (2008) 266–271.
[29] T.E. Sheridan, J. Goree, Y.T. Chiu, R.L. Rairden, J.A. Kiessling, Observation of dust shedding from material bodies in a plasma, J. Geophys. Res. 97 (1992) 2935.
[30] T.M. Flanagan, J. Goree, Dust release from surfaces exposed to plasma, Phys. Plasmas 13 (2006) 123504.
[31] X. Wang, M. Horányi, S. Robertson, Investigation of dust transport on the lunar surface in a laboratory plasma with an electron beam, J. Geophys. Res. 115 (2010). A11102.
[32] T.E. Sheridan, A. Hayes, Charge fluctuations for particles on a surface exposed to plasma, Appl. Phys. Lett. 98 (2011), 091501.
[33] L.C.J. Heijmans, S. Nijdam, Dust on a surface in a plasma: a charge simulation,, Phys. Plasmas 23 (2016), 043703.
[34] X. Wang, J. Schwan, H.-W. Hsu, E. Grün, M. Horányi, Dust charging and transport on airless planetary bodies, Geophys. Res. Lett. 43 (2016) 6103–6110.
[35] J. Schwan, X. Wang, H.-W. Hsu, E. Grün, M. Horányi, The charge state of electrostatically transported dust on regolith surfaces,, Geophys. Res. Lett. 44 (2017) 3059–3065.
[36] N. Hood, A. Carroll, R. Mike, X. Wang, J. Schwan, H.-W. Hsu, M. Horányi, Laboratory investigation of rate of electrostatic dust lofting over time on airless planetary bodies, Geophys. Res. Lett. 45 (2018), 13,206–13,212.
[37] A. Dove, M. Horanyi, S. Robertson, X. Wang, Laboratory investigation of the effect of surface roughness on photoemission from surfaces in space, Planet. Space Sci. 156 (2018) 92–95.
[38] N.C. Orger, K. Toyoda, H. Masui, M.G. Cho, Experimental investigation on silica dust lofting due to charging within micro-cavities and surface electric field in the vacuum chamber, Adv. Space Res. 63 (2019) 3270–3288.
[39] A. Carroll, N. Hood, R. Mike, X. Wang, H.-W. Hsu, M. Horányi, Laboratory measurements of initial launch velocities of electrostatically lofted dust on airless planetary bodies, Icarus 352 (2020) 113972.